Generalized Dalitz Plot analysis of the near threshold $pp \rightarrow ppK^+K^-$ reaction in view of the K^+K^- final state interaction

M. Silarski,[1] P. Moskal,[1,2,*] E. Czerwiński,[1,2] R. Czyżykiewicz,[1] D. Gil,[1] D. Grzonka,[2] L. Jarczyk,[1] B. Kamys,[1] A. Khoukaz,[3] J. Klaja,[1,2] P. Klaja,[1,2] W. Krzemień,[1,2] W. Oelert,[2] J. Ritman,[2] T. Sefzick,[2] M. Siemaszko,[4] J. Smyrski,[1] A. Täschner,[3] P. Winter,[5] M. Wolke,[2] P. Wüstner,[2] M. Zieliński,[1] W. Zipper,[4] and J. Zdebik[1]

[1]*Institute of Physics, Jagiellonian University, PL-30-059 Cracow, Poland*
[2]*Institute for Nuclear Physics and Jülich Center for Hadron Physics,*
Research Center Jülich, D-52425 Jülich, Germany
[3]*IKP, Westfälische Wilhelms-Universität, D-48149 Münster, Germany*
[4]*Institute of Physics, University of Silesia, PL-40-007 Katowice, Poland*
[5]*University of Illinois at Urbana-Champaign, Urbana, IL 61801, USA*
(Dated: September 22, 2009)

The excitation function for the $pp \rightarrow ppK^+K^-$ reaction revealed a significant enhancement close to threshold which may plausibly be assigned to the influence of the pK^- and K^+K^- final state interactions. In an improved reanalysis of COSY-11 data for the $pp \rightarrow ppK^+K^-$ reaction at excess energies of Q = 10 MeV and 28 MeV including the proton-K^- interaction the enhancement is confirmed. Invariant mass distributions for the two- and three-particle subsystems allow to test at low excess energies the ansatz and parameters for the description of the interaction in the ppK^+K^- system as derived from the COSY-ANKE data. Finally, based for the first time on the low energy K^+K^- invariant mass distributions and the generalized Dalitz plot analysis, we estimate the scattering length for the K^+K^- interaction to be $|Re(a_{K^+K^-})| = 0.5^{+4.0}_{-0.5}$ fm and $Im(a_{K^+K^-}) = 3.0 \pm 3.0$ fm.

I. INTRODUCTION

The basic motivation for investigating the $pp \rightarrow ppK^+K^-$ reaction near the kinematical threshold is comprehensively reviewed in [1], as an attempt to understand the nature of the scalar resonances $f_0(980)$ and $a_0(980)$, whose masses are very close to the sum of the K^+ and K^- masses. Besides the standard interpretation as $q\bar{q}$ mesons [2], these resonances were also proposed to be $qq\bar{q}\bar{q}$ states [3], $K\bar{K}$ molecules [4, 5], hybrid $q\bar{q}$/meson-meson systems [6] or even quark-less gluonic hadrons [7]. The strength of the $K\bar{K}$ interaction is a crucial quantity regarding the formation of a $K\bar{K}$ molecule, whereas the KN interaction is of importance in view of the vigorous discussion concerning the structure of the excited hyperon $\Lambda(1405)$ which is considered as a three quark system or as a KN molecular state [8]. Additionally, these interactions appear to be very important also with respect to other phenomena, like possible kaon condensation in neutron stars [9], or production of strange particles immersed in a dense nuclear medium studied by means of heavy ion collisions [10, 11, 12, 13].

Measurements of the near threshold $pp \rightarrow ppK^+K^-$ reaction have been made possible by beams of low emittance and small momentum spread available at storage ring facilities, in particular at the cooler synchrotron COSY at the research center in Jülich in Germany [14].

A precise determination of the collision energy, in the order of fractions of MeV, permitted to deal with the rapid growth of cross sections [15] and thus to take advantage of the threshold kinematics like, e.g., full phase space coverage achievable with dipole magnetic spectrometers being rather limited in geometrical acceptance. Early experiments on K^+K^- pair production at COSY conducted by the COSY-11 collaboration revealed, however, that the total cross section at threshold is by more than seven orders of magnitude smaller than the total proton-proton production cross section making the study difficult due to low statistics [16, 17, 18]. A possible influence from the f_0 or a_0 mesons on the K^+K^- pair production appeared to be too weak to be distinguished from the direct production of these mesons based on the COSY-11 data [17]. Recent results obtained by the ANKE collaboration with much higher statistics can also be explained without the need of including the scalars f_0 or a_0 [19, 20]. However, the combined systematic collection of data below [16, 17, 18] and above [19, 21] the ϕ meson threshold reveal a significant signal in the shape of the excitation function which may be due to the K^-p and perhaps also to the K^+K^- interaction. This signal is based on the COSY-11 data which, as indicated by authors of article [19], were analyzed calculating the acceptance without the inclusion of the pK^- interaction. Therefore a more detailed analysis of the COSY-11 data at excess energies of Q = 10 MeV and 28 MeV including now studies of both the differential cross section distributions and the strength of the final state interaction between the K^+ and K^- mesons was performed. The analysis is based

*Electronic address: p.moskal@fz-juelich.de

on a generalization of the Dalitz plot for four particles as proposed by Goldhaber *et al.* [22, 23, 24].

II. EXCITATION FUNCTION FOR THE NEAR THRESHOLD $pp \rightarrow ppK^+K^-$ REACTION

The measurements of the $pp \rightarrow ppK^+K^-$ reaction were conducted at low excess energies by the collaborations ANKE [19], COSY-11 [16, 17, 18] and DISTO [21]. The achieved results are presented in Fig. 1 together with curves representing three different theoretical expectations [19] normalized to the DISTO data point at Q = 114 MeV. The dashed curve represents the energy dependence from four-body phase space when we assume that there is no interaction between particles in the final state. These calculations differ from the experimental data by two orders of magnitude at Q = 10 MeV and by a factor of about five at Q = 28 MeV. Hence, it is obvious, that effects of final state interactions cannot be neglected in the ppK^+K^- system [25]. Inclusion of the
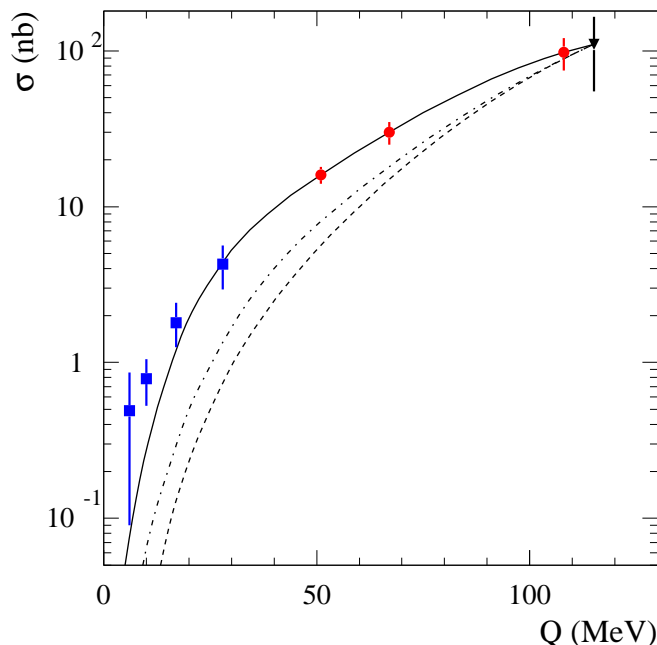

FIG. 1: (Color online) Excitation function for the $pp \rightarrow ppK^+K^-$ reaction. Triangle and circles represent the DISTO and ANKE measurements, respectively. The four points close to the threshold are results from the COSY-11 measurements. The curves are described in the text.

pp–FSI (dashed-dotted line in Fig. 1), by folding its parameterization known from the three body final state [26] with the four body phase space, is closer to the experimental data, but does not fully account for the difference [18]. The enhancement may be due to the influence of pK and K^+K^- interaction which was neglected in the calculations. Indeed, as shown by authors of reference [19, 20] the inclusion of the pK^-–FSI (solid line) reproduces the experimental data for excess energies down

to Q = 28 MeV. These calculations of the cross section were accomplished under the assumption that the overall enhancement factor, originating from final state interaction in the ppK^+K^- system, can be factorised into enhancements in the pp and two pK^- subsystems [19]:

$$F_{FSI} = F_{pp}(q) \cdot F_{p_1 K^-}(k_1) \cdot F_{p_2 K^-}(k_2) , \qquad (1)$$

where k_1, k_2 and q stand for the relative momenta of the particles in the first pK^- subsystem, second pK^- subsystem and pp subsystem, respectively. The factors describing the enhancement originating from the pK^-–FSI are parametrized using the scattering length approximation. It is important to note that the inclusion of the pp and pK^- final state interaction is not sufficient to describe the data very close to threshold (see Fig. 1). This enhancement may be due to the influence of the K^+K^- interaction, which was neglected in the calculations [44]. However, as pointed out in Ref. [19] the observed increase of the total cross section near threshold may be due to the neglect of the pK^-–FSI in the calculations of the COSY-11 acceptance. As a consequence the extracted cross sections would decrease, if this interaction was taken into account during the analysis of the experimental data. This concern encouraged us to check quantitatively the influence of the interaction in the pK^- subsystem on the acceptance of the detection setup. In addition, absolute values for the differential distributions of the pK and ppK invariant masses were extracted and generalized Dalitz plot analysis of the data in view of the K^+K^- interaction, was performed.

III. MEASUREMENTS OF THE $pp \rightarrow ppK^+K^-$ REACTION PERFORMED WITH THE COSY-11 MAGNETIC SPECTROMETER

The measurements of the $pp \rightarrow ppK^+K^-$ reaction close to threshold have been conducted using the cooler synchrotron COSY [14] and the COSY-11 detector system [27] shown schematically in Fig. 2. The target, being a beam of H_2 molecules grouped to clusters of up to 10^5 atoms [28], crosses perpendicularly the proton beam circulating in the ring. If a collision of protons leads to the production of a K^+K^- meson pair, then the reaction products, having smaller momenta than the circulating beam, are directed by the magnetic dipole field towards the COSY-11 detection system and leave the vacuum chamber through a thin exit foil [27]. Tracks of positively charged particles, registered by drift chambers, are traced back through the magnetic field to the nominal interaction point leading to a momentum determination. The knowledge of the momentum combined with an independent measurement of the velocity, performed by means of the scintillation detectors S1 and S3, permits to identify the registered particles and to determine their four momentum vectors. Knowing both the four momenta of the three positively charged ejectiles and the proton
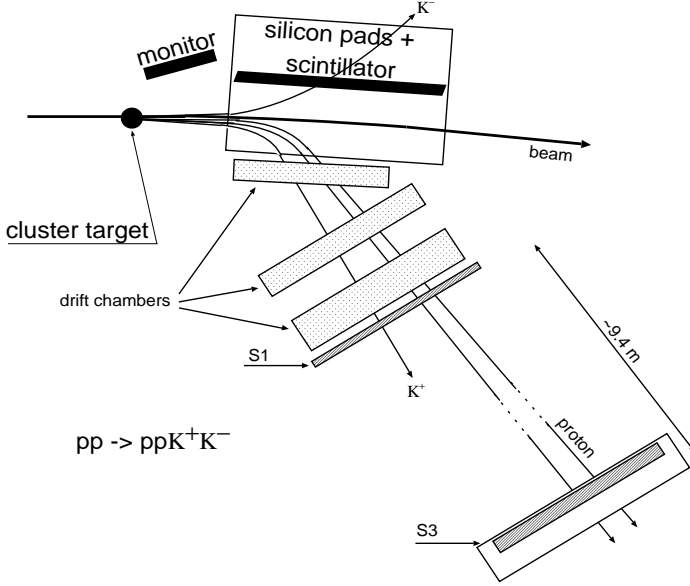
FIG. 2: Schematic view of the COSY-11 detector with a typical event of the $pp \to ppK^+K^-$ reaction channel. For the description see text.

beam momentum one can calculate the mass of the unobserved system X^-. In the case of the $pp \to ppK^+K^-$ reaction this should correspond to the mass of the K^- meson, but we observe also background originating partly from the $pp \to pp\pi^+X^-$ reaction, where the π^+ was misidentified as a K^+ meson, and in part due to the K^+ meson being associated with the hyperons $\Lambda(1405)$ or $\Sigma(1385)$ production [17, 18]. This background, however, can be completely removed by demanding a signal in the silicon pad detectors (mounted inside the dipole) at the position where the K^- meson originating from the $pp \to ppK^+K^-$ reaction is expected. This clear identification allows to select the $pp \to ppK^+K^-$ events and to determine the total and differential cross sections. A more detailed description of the experiment and data evaluation is given in [16, 17, 18, 27, 29].

IV. DIFFERENTIAL OBSERVABLES FOR COSY-11 DATA AT Q = 10 MeV AND Q = 28 MeV

In order to check the sensitivity of the result to the assumption of the pK^- final state interaction we derived the distributions of the differential cross section assuming that the acceptance depends only on the pp–FSI [45]. Then we calculated the acceptance with inclusion of the pp– and pK^-–FSI, and derived analogous distributions. In this calculations we assumed the factorisation of the final state interaction given by Eq. 1 and used the pK^- scattering length $a_{pK^-} = (0 + 1.5i)$ fm [19]. The results are presented in Fig. 3 for data at Q = 10 MeV and in Fig. 4 for Q = 28 MeV. The distributions obtained under

TABLE I: The differential cross sections of the $pp \to ppK^+K^-$ reaction as a function of invariant masses for different subsystems. The values of M_{ij} denote the center of the invariant mass bins of 2.5 MeV/c^2 and 7.0 MeV/c^2 width for Q = 10 MeV and Q = 28 MeV, respectively.

Q = 10 MeV		Q = 28 MeV	
M_{pp} $\left(\frac{\text{GeV}}{\text{c}^2}\right)$	$\frac{d\sigma}{dM_{pp}}$ $\left(\frac{\text{nb}}{\text{GeV/c}^2}\right)$	M_{pp} $\left(\frac{\text{GeV}}{\text{c}^2}\right)$	$\frac{d\sigma}{dM_{pp}}$ $\left(\frac{\text{nb}}{\text{GeV/c}^2}\right)$
1.8778	216 ± 53	1.880	388 ± 92
1.8803	106 ± 34	1.887	346 ± 87
1.8828	43 ± 22	1.894	148 ± 67
1.8853	14 ± 14	1.901	48 ± 48
M_{pK^+} $\left(\frac{\text{GeV}}{\text{c}^2}\right)$	$\frac{d\sigma}{dM_{pK^+}}$ $\left(\frac{\text{nb}}{\text{GeV/c}^2}\right)$	M_{pK^+} $\left(\frac{\text{GeV}}{\text{c}^2}\right)$	$\frac{d\sigma}{dM_{pK^+}}$ $\left(\frac{\text{nb}}{\text{GeV/c}^2}\right)$
1.4332	107 ± 34	1.435	255 ± 72
1.4357	122 ± 39	1.442	261 ± 76
1.4382	125 ± 42	1.449	287 ± 83
1.4407	32 ± 21	1.456	63 ± 37
M_{pK^-} $\left(\frac{\text{GeV}}{\text{c}^2}\right)$	$\frac{d\sigma}{dM_{pK^-}}$ $\left(\frac{\text{nb}}{\text{GeV/c}^2}\right)$	M_{pK^-} $\left(\frac{\text{GeV}}{\text{c}^2}\right)$	$\frac{d\sigma}{dM_{pK^-}}$ $\left(\frac{\text{nb}}{\text{GeV/c}^2}\right)$
1.4332	173 ± 47	1.435	581 ± 117
1.4357	145 ± 42	1.442	135 ± 56
1.4382	36 ± 21	1.449	97 ± 46
1.4407	13 ± 11	1.456	25 ± 21
$M_{K^+K^-}$ $\left(\frac{\text{GeV}}{\text{c}^2}\right)$	$\frac{d\sigma}{dM_{K^+K^-}}$ $\left(\frac{\text{nb}}{\text{GeV/c}^2}\right)$	$M_{K^+K^-}$ $\left(\frac{\text{GeV}}{\text{c}^2}\right)$	$\frac{d\sigma}{dM_{K^+K^-}}$ $\left(\frac{\text{nb}}{\text{GeV/c}^2}\right)$
0.9887	169 ± 44	0.991	221 ± 70
0.9912	174 ± 51	0.998	454 ± 114
0.9937	35 ± 21	1.005	230 ± 70
0.9962	0 ± 9	1.012	38 ± 22
M_{ppK^+} $\left(\frac{\text{GeV}}{\text{c}^2}\right)$	$\frac{d\sigma}{dM_{ppK^+}}$ $\left(\frac{\text{nb}}{\text{GeV/c}^2}\right)$	M_{ppK^+} $\left(\frac{\text{GeV}}{\text{c}^2}\right)$	$\frac{d\sigma}{dM_{ppK^+}}$ $\left(\frac{\text{nb}}{\text{GeV/c}^2}\right)$
2.3715	0 ± 13	2.374	20 ± 20
2.3740	68 ± 28	2.381	61 ± 36
2.3765	164 ± 43	2.388	247 ± 72
2.3790	99 ± 38	2.395	566 ± 121
M_{ppK^-} $\left(\frac{\text{GeV}}{\text{c}^2}\right)$	$\frac{d\sigma}{dM_{ppK^-}}$ $\left(\frac{\text{nb}}{\text{GeV/c}^2}\right)$	M_{ppK^-} $\left(\frac{\text{GeV}}{\text{c}^2}\right)$	$\frac{d\sigma}{dM_{ppK^-}}$ $\left(\frac{\text{nb}}{\text{GeV/c}^2}\right)$
2.3715	60 ± 30	2.374	204 ± 68
2.3740	115 ± 39	2.381	284 ± 79
2.3765	127 ± 39	2.388	176 ± 63
2.3790	87 ± 31	2.395	216 ± 69

both assumptions are almost identical, which shows that the acceptance of the COSY-11 detection setup is only very weakly sensitive to the interaction between K^- and protons. Thus, the observed enhancement in the excitation function cannot be explained by approximations in the determination of the detection efficiency as suspected by [19]. This justifies the assumption made in the original analysis, where the efficiency was calculated taking into account the pp–FSI only.

The derived values of differential cross sections are listed in Table I. This result constitutes an additional information to the total cross sections published previously [18]. The values of the cross sections in the former analysis [18] were determined using the total number of events identified as a $pp \to ppK^+K^-$ reaction and the total acceptance of the COSY-11. Now after the determination of the absolute values for the differential distributions one can calculate the total cross sections in a less model dependent manner regardless of the assumption of the
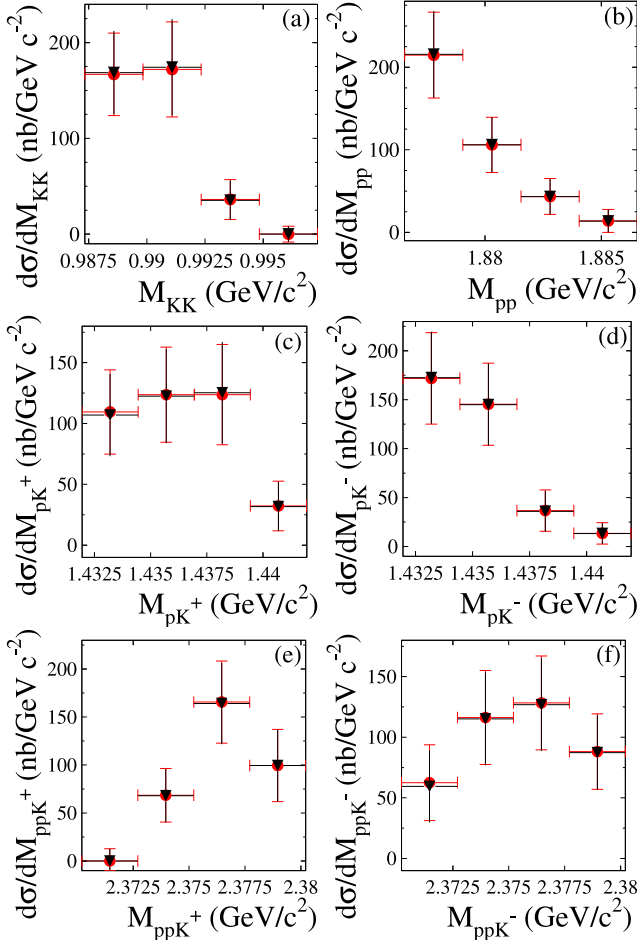
FIG. 3: (Color online) Differential cross sections for the $pp \rightarrow ppK^+K^-$ reaction at Q = 10 MeV. Circles and dashed bars (in black) denote spectra where the acceptance was determined taking into account only the pp–FSI, and triangles with solid bars (in red) denote results where pp– and pK^-–FSI was taken into account in the acceptance calculations. They are hardly distinguishable. Vertical bars indicate statistical errors, whereas the horizontal bars stand for the invariant mass intervals for which the cross section values were established.

pp–FSI. The cross sections, calculated for both excess energies as an integral of the M_{pp} distribution derived with the inclusion of the pK^-–FSI in the acceptance calculations:

$$\sigma_{\text{tot}} = \int \frac{d\sigma}{dM_{pp}} dM_{pp} \ ,$$

amount to $\sigma_{\text{tot}} = (0.95 \pm 0.17)$ nb for measurement at Q = 10 MeV and $\sigma_{\text{tot}} = (6.5 \pm 1.1)$ nb for Q = 28 MeV. These results are statistically consistent with the previously evaluated total cross sections. However, the values extracted in the actual analysis with smaller error bars are larger by about 20% for Q = 10 MeV and 50% for Q = 28 MeV, which strengthens the confidence to the observed enhancement at threshold.

The determination of the absolute values for the differential cross sections permitted us to establish the absolute
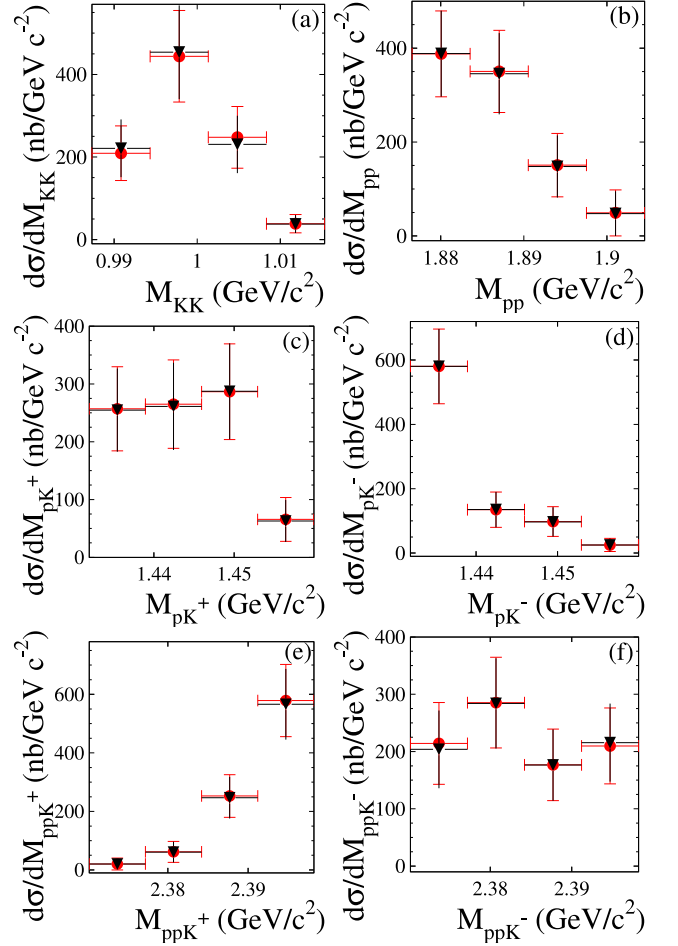
FIG. 4: (Color online) Differential cross sections for the $pp \rightarrow ppK^+K^-$ reaction at Q = 28 MeV. For the description see caption of Fig. 3

values for the following ratios at the close to threshold region [46]:

$$R_{pK} = \frac{d\sigma/dM_{pK^-}}{d\sigma/dM_{pK^+}} \ ,$$

$$R_{ppK} = \frac{d\sigma/dM_{ppK^-}}{d\sigma/dM_{ppK^+}} \ .$$

If pK^+ and pK^- interactions were the same, the distribution of R_{pK} as well as R_{ppK} should be flat and equal to unity. But as one can see in Fig. 5 and as presented already in the previous publication by COSY-11 [18] and ANKE [19] for both excess energies R_{pK} is far from being constant and increases towards the lower M_{pK} invariant masses. This effect might be due to the influence of the pK^- final state interaction. Similarly the distributions of R_{ppK} differs from expectations assuming only FSI in the pp system. This is a confirmation of effects observed also by the ANKE collaboration at higher excess energies [19]. The determination of the absolute values of the ratios R_{pK} and R_{ppK} allows to compare the parameters of the scattering length a_{pK^-} derived by the ANKE group
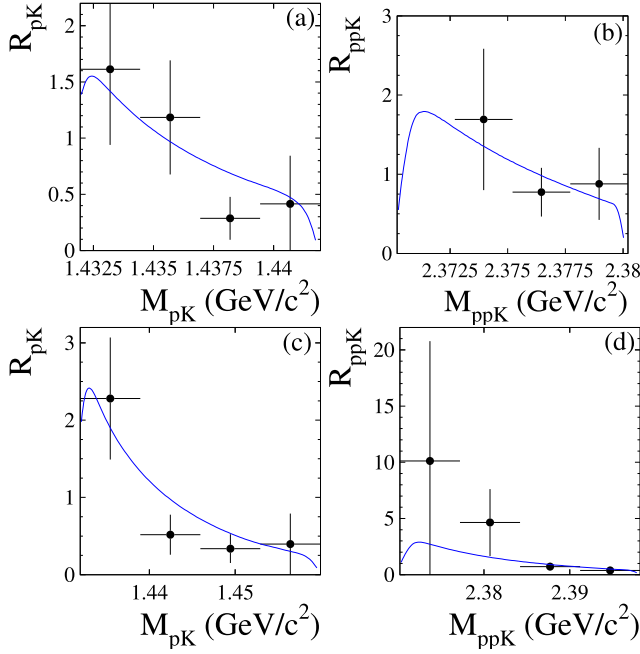
FIG. 5: (Color online) The distributions of the absolute values of ratios R_{pK} and R_{ppK} for data at Q = 10 MeV ((a) and (b)) and Q = 28 MeV ((c) and (d)). Solid curves represent theoretical expectations calculated taking into account pp and pK^- final state interaction. It should be stressed that the absolute values are not fitted, but they are result of the model and used parameters [19].

(from data at excess energies above the ϕ meson production threshold), to the present data near the K^+K^- threshold. As demonstrated in Fig. 5, simulations taking into account the pK^- final state interaction with the scattering length $a_{pK^-} = (0 + 1.5i)$ fm determined by the ANKE group from data at significantly higher excess energies reproduce very well the distributions of R_{pK} and R_{ppK} near the threshold.

V. ANALYSIS OF THE K^+K^- FINAL STATE INTERACTION

A factorization ansatz for the pp and pK^- interaction underestimate the excitation function for the $pp \to ppK^+K^-$ reaction very close to threshold indicating that in this energy region the influence of the K^+K^- interaction is significant and cannot be neglected. The interaction may manifest itself even stronger in the distributions of the differential cross sections [15]. This observation demands an analysis of the double differential cross sections for the low energy data at Q = 10 MeV (27 events) and Q = 28 MeV (30 events), in spite of the quite low statistics available.

A. Generalization of the Dalitz plot: Goldhaber approach

There are many different types of generalizations of the Dalitz plot for four-body final states [34, 35]. Here a generalization proposed by Goldhaber is presented [22, 23, 24].

Consider a reaction like $a + b \longrightarrow 1 + 2 + 3 + 4$ yielding four particles with masses m_i and total energy $\sqrt{s}$ in the centre-of-mass frame. The probability, that the momentum of the ith particle is in a range d^3p_i is given by:

$$d^{12}P = d^3p_1 d^3p_2 d^3p_3 d^3p_4 \frac{1}{16E_1E_2E_3E_4}$$
$$\times \delta^3\left(\sum_{j=1}^{4} \mathbf{p_j}\right) \delta\left(\sum_{j=1}^{4} E_j - \sqrt{s}\right) |M|^2 , \quad (2)$$

where $E_i = \sqrt{\mathbf{p_i^2} + m_i^2}$ denotes the energy of the ith particle (c = 1) and M denotes the invariant matrix element for the process. Assuming that the matrix element M depends only on the invariant masses of the two- and three particle subsystems [34], the distribution given by Eq. 2 can be expressed in some choice of five independent invariant masses [47]. An especially convenient choice is $M_{12}^2, M_{34}^2, M_{14}^2, M_{124}^2$, and M_{134}^2 [34]. Using such variables, after integrations, one obtains an event distribution in the following form:

$$d^5P = \frac{\pi^2}{8s} |M|^2 \frac{1}{\sqrt{-B}} dM_{12}^2 dM_{34}^2 dM_{14}^2 dM_{124}^2 dM_{134}^2 , \quad (3)$$

where B is a function of the invariant masses with the exact form to be found in Nyborg's work [34]. An advantage of the choice of mass variables used here is the high symmetry of the function B [34], which is very usefull in the consideration of the boundary of the kinematically allowed region in the $\left(M_{12}^2, M_{34}^2, M_{14}^2, M_{124}^2, M_{134}^2\right)$ space defined by B = 0. If we additionally change the integration variables to invariant masses the projection of the physical region on the (M_{12}, M_{34})-plane gives a convenient and simple distribution, which can be used to analyse the final state interaction in the same way as in case of three particles. Such an analysis was originally made by Goldhaber et al. in 1963 [22, 23] and is called Goldhaber plot. As it is shown in Fig. 6 the kinematically allowed region in the Goldhaber plot is a right isosceles triangle within which the area (contrary to the Dalitz plot) is not proportional to the phase space volume [34]. Moreover, even in the case of the absence of any final state interaction the density of events on the Goldhaber plot is not homogeneous. However, it is still a very convenient tool due to its lorentz invariance and simple boundary equations [34]:

$$M_{12}+M_{34}=\sqrt{s} \, , \; M_{12}=m_1+m_2 \, , \text{and} \; M_{34}=m_3+m_4 \, .$$
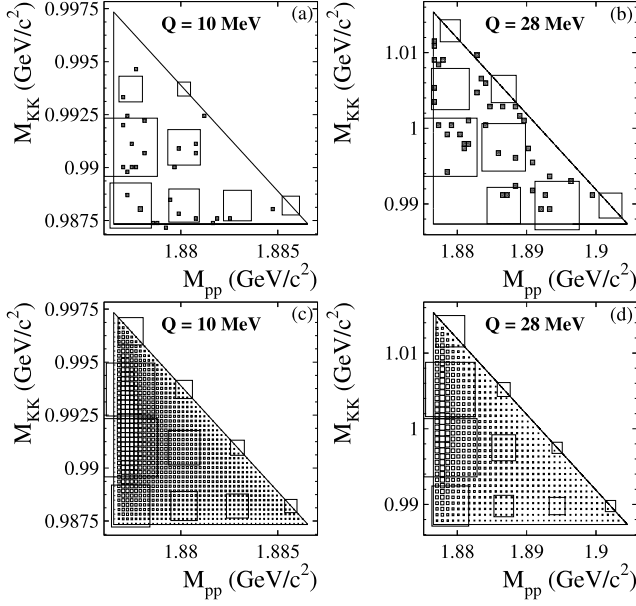
FIG. 6: Goldhaber plots for the $pp \rightarrow ppK^+K^-$ reaction. The solid lines of the triangles show the kinematically allowed boundaries. Raw data are shown in Figs. (a) and (b) as black points. The superimposed squares represent the same distributions but binned into intervals of $\Delta M = 2.5$ MeV/c^2 ($\Delta M = 7$ MeV/c^2) widths for an excess energy of $Q = 10$ MeV (28 MeV), respectively. The size of the square is proportional to the number of entries in a given interval. In Figs. (c) and (d) Monte Carlo results are presented. In the simulated distributions both the pp and the pK^-–FSI are taken into account.

B. Determination of the K^+K^- scattering length

Complementary to previous derivations [36, 37, 38, 39] here we estimate the K^+K^- scattering length directly from the low energy differential mass distributions of K^+K^- and pp pairs from the ppK^+K^- system produced at threshold. The raw data (represented by black points in Figs. 6(a) and 6(b)) were first binned into intervals of $\Delta M = 2.5$ MeV/c^2 width for the measurement at $Q = 10$ MeV and intervals of $\Delta M = 7$ MeV/c^2 for the data at $Q = 28$ MeV, and then for each bin corrected for the acceptance and detection efficiency of the COSY-11 facility [40]. The resulting Goldhaber plots are presented together with the raw distributions in Figs. 6(a) and 6(b). Figures 6(c) and 6(d) show corresponding distributions simulated with Monte Carlo method taking into account the pp and pK^- interaction according to the factorization ansatz [19].

In order to estimate the strength of the K^+K^- interaction, the derived cross sections were compared to results of simulations generated with various parameters of the K^+K^- interaction taking into account strong final state interaction in the pp and pK^- subsystems. To describe the experimental data in terms of final state interactions between i) the two protons, ii) the K^- and protons and
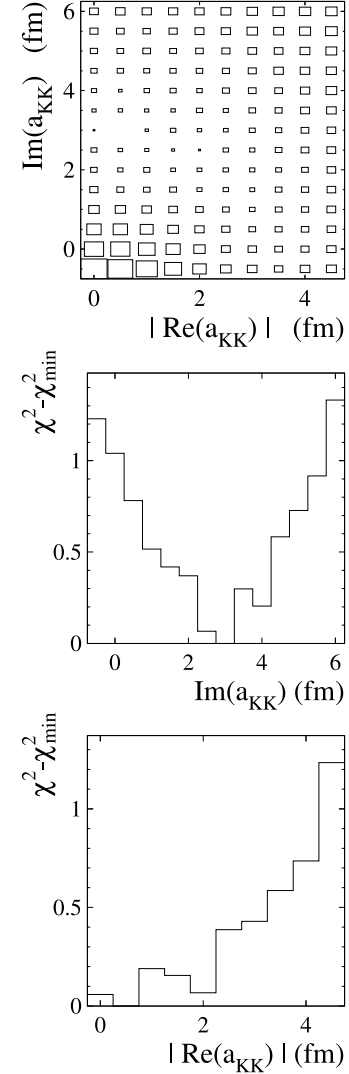

FIG. 7: χ^2 - χ^2_{min} distribution as a function of $|Re(a_{K^+K^-})|$ and $Im(a_{K^+K^-})$. χ^2_{min} denotes the absolute minimum with respect to parameters α, $|Re(a_{K^+K^-})|$, and $Im(a_{K^+K^-})$.

iii) the K^+ and K^-, the K^+K^- enhancement factor was introduced such that Eq. 1 changes to:

$$F_{FSI} = F_{pp}(q) \cdot F_{p_1 K^-}(k_1) \cdot F_{p_2 K^-}(k_2) \cdot F_{K^+K^-}(k_3) . \quad (4)$$

As for the case of the pK^-–FSI, the $F_{K^+K^-}$ was calculated in the scattering length approximation:

$$F_{K^+K^-} = \frac{1}{1 - i \, k_3 \, a_{K^+K^-}} , \quad (5)$$

where $a_{K^+K^-}$ is the effective K^+K^- scattering length and k_3 stands for the relative momentum of the kaons in their rest frame. Using this parametrization we compared the experimental event distributions to the results of Monte Carlo simulations treating the K^+K^- scattering length as an unknown parameter, which has to be determined. In order to estimate the real and imaginary part of $a_{K^+K^-}$ we constructed the Poisson likeli-

hood χ^2 statistic derived from the maximum likelihood method [41, 42]:

$$\chi^2 \left(a_{K^+K^-}, \alpha\right) = 2 \cdot \sum_i \left[\alpha N_i^s - N_i^e + N_i^e \ln\left(\frac{N_i^e}{\alpha N_i^s}\right)\right] , \ (6)$$

where N_i^e denotes the number of events in the ith bin of the experimental Goldhaber plot, N_i^s stands for the content of the same bin in the simulated distributions, and α is the normalization factor. The data collected at both excess energies have been analysed simultaneously. The obtained χ^2 distributions (suppressed by its minimum value) as a function of the real and imaginary part of the K^+K^- scattering length are presented in Fig. 7. The best fit to the experimental data corresponds to $|Re(a_{K^+K^-})| = 0.5 \ ^{+4}_{-0.5}$ fm and $Im(a_{K^+K^-}) = 3 \pm 3$ fm. The final state interaction enhancement factor $F_{K^+K^-}$ in the scattering length approximation is symmetrical with respect to the sign of $Re(a_{K^+K^-})$, therefore only its absolute value can be determined.

VI. CONCLUSIONS

In conclusion, the more detailed analysis of the COSY-11 data with inclusion of the pK^- final state interaction did not change significantly the result of the previous analysis [18]. Moreover, the new more precise determination of the total cross sections from the differential M_{pp} distributions even increased the enhancement at threshold.

In addition the analysis of the $pp \rightarrow ppK^+K^-$ reaction has been extended to the determination of differential cross sections in view of the K^+K^- final state interaction. The extracted K^+K^- scattering length amounts to:

$$a_{K^+K^-} = [(0.5 \ ^{+4}_{-0.5}) + i(3 \pm 3)] \ \text{fm.}$$

Due to the low statistics the uncertainties are rather large. In this analysis we cannot distinguish between the isospin I = 0 and I = 1 states of the K^+K^- system. However, as pointed out in [43], the production with I = 0 is dominant in the $pp \rightarrow ppK^+K^-$ reaction independent of the exact values of the scattering lengths.

Regarding the comparison of the interactions in the pK^-, pK^+, ppK^- and ppK^+ subsystems, the absolute ratios determined from the COSY-11 data measured at Q = 10 MeV and Q = 28 MeV are consistent with the predictions based on the parametrization introduced in reference [19] and on the values of the scattering length a_{pK^-} extracted from the ANKE data at higher excess energies [19].

[1] W. Oelert, *in Proceedings of the Workshop on Meson Production, Interaction and Decay, Cracow, 1991,* World Scientific, Singapore (1991) p. 199.
[2] D. Morgan, M. R. Pennington, Phys. Rev. D **48**, 1185 (1993).
[3] R. L. Jaffe, Phys. Rev. D **15**, 267 (1977).
[4] D. Lohse *et al.*, Nucl. Phys. **A516**, 513 (1990).
[5] J. D. Weinstein, N. Isgur, Phys. Rev. D **41**, 2236 (1990).
[6] E. Van Beveren, *et al.*, Z. Phys. C **30**, 615 (1986).
[7] R. L. Jaffe, K. Johnson, Phys. Lett. **B60**, 201 (1976).
[8] N. Kaiser, P. B. Siegel, W. Weise, Nucl. Phys. **A594**, 325 (1995).
[9] G. Q. Li, C.-H. Lee, G. E. Brown, Nucl. Phys. **A625**, 372 (1997).
[10] P. Senger *et al.*, Phys. Rev. C **75**, 024906 (2007).
[11] F. Laue *et al.*, Phys. Rev. Lett. **82**, 1640 (1999).
[12] R. Barth *et al.*, Phys. Rev. Lett. **78**, 4007 (1997).
[13] M. Menzel *et al.*, Phys. Lett. **B495**, 26 (2000).
[14] D. Prasuhn *et al.*, Nucl. Instrum. Methods Phys. Res. A **441**, 167 (2000); R. Maier, *ibid.* **390**, 1 (1997).
[15] P. Moskal, M. Wolke, A. Khoukaz, W. Oelert, Prog. Part. Nucl. Phys. **49**, 1 (2002).
[16] M. Wolke, PhD thesis, IKP Jül-3532 (1997).
[17] C. Quentmeier *et al.*, Phys. Lett. **B515**, 276 (2001).
[18] P. Winter *et al.*, Phys. Lett. **B635**, 23 (2006).
[19] Y. Maeda *et al.*, Phys. Rev. C **77**, 01524 (2008).
[20] C. Wilkin, AIP Conf. Proc. **950**, 23 (2007).
[21] F. Balestra *et al.*, Phys. Lett. **B468**, 7 (1999).
[22] W. Chinowsky, G. Goldhaber, S. Goldhaber, W. Lee, T. O'Halloran, Phys. Rev. Lett. **9**, 330 (1962).
[23] W. Chinowsky, G. Goldhaber, S. Goldhaber, W. Lee, T. O'Halloran, Phys. Rev. Lett. **6**, 62 (1963).
[24] C. Wilkin, remarks at the Symposium on Meson Physics, Cracow (2007).
[25] W. Oelert *et al.*, Int. J. of Mod. Phys. A **22**, 502 (2007).
[26] P. Moskal *et al.*, Phys. Lett. **B482**, 356 (2000).
[27] S. Brauksiepe *et al.*, Nucl. Instrum. Methods Phys. Res. A **376**, 397 (1996).
[28] H. Dombrowski *et al.*, Nucl. Instrum. Methods Phys. Res. A **386**, 228 (1997).
[29] P. Moskal *et al.*, J. Phys. G **28**, 1777 (2002).
[30] H. P. Noyes, H. M. Lipinski, Phys. Rev. C **4**, 995 (1971).
[31] H. P. Noyes, Ann. Rev. Nucl. Sci. **22**, 465 (1972).
[32] J. P. Naisse, Nucl. Phys. **A278**, 506 (1977).
[33] P. Moskal, *e-Print Archive*: hep-ph/0408162.
[34] P. Nyborg *et al.*, Phys. Rev. **140**, 914 (1965).
[35] D. Chodrow, Nuovo Cimento **50**, 674 (1967).
[36] R. Kamiński, L. Leśniak, Phys. Rev. C **54**, 2264 (1995).

[37] V. Baru *et al.*, Phys. Lett. **B586**, 53 (2004).

[38] S. Teige *et al.*, Phys. Rev. D **59**, 012001 (2001).

[39] D. V. Bugg, V. V. Anisovich, A. Sarantsev, B.S. Zou, Phys. Rev. D **50**, 4412 (1994).

[40] M. Silarski, arXiv:0809.0837v1; FZ-Jülich report, Jül-4278, (2008).

[41] S. Baker, R.D. Cousins, Nucl. Instrum. Methods Phys. Res. A **221**, 437 (1984).

[42] G. J. Feldman, R. D. Cousins, Phys. Rev. D **57**, 3873 (1998).

[43] A. Dzyuba *et al.*, Phys. Lett. **B668**, 315 (2008).

[44] It is worth mentioning, that in the calculations also the pK^+ interaction was neglected. It is repulsive and weak and hence it can be interpreted as an additional attraction in the pK^- system [19].

[45] In all calculations we used the following parametrization of the proton-proton scattering amplitude:

$$F_{pp} = \frac{e^{-i\delta_{pp}(^1\mathrm{S}_0)} \cdot \sin\delta_{pp}(^1\mathrm{S}_0)}{C \cdot \mathrm{q}} \ ,$$

where C stands for the square root of the Coulomb penetration factor [26]. The parameter $\delta_{pp}(^1\mathrm{S}_0)$ denotes

the phase-shift calculated according to the modified Cini-Fubini-Stanghellini formula with the Wong-Noyes Coulomb correction [30, 31, 32]. A more detailed description of this parametrization can be found in references [26, 30, 31, 32, 33].

[46] In the former analysis only the shape of the ratios was established.

[47] Actually for four particles in the final state we have six two-particle and four three-particle invariant masses. But only five of them are independent due to following relations [34]:

$$\sum_{i,j=1(i>j)}^{4} M_{ij}^2 = s + 2\sum_{i=1}^{4} m_i^2 \ ,$$

$$M_{123}^2 = M_{12}^2 + M_{23}^2 + M_{13}^2 - m_1^2 - m_2^2 - m_3^2 \ ,$$
$$M_{134}^2 = M_{13}^2 + M_{34}^2 + M_{14}^2 - m_1^2 - m_3^2 - m_4^2 \ ,$$
$$M_{124}^2 = M_{12}^2 + M_{24}^2 + M_{14}^2 - m_1^2 - m_2^2 - m_4^2 \ ,$$
$$M_{234}^2 = M_{22}^2 + M_{34}^2 + M_{24}^2 - m_2^2 - m_3^2 - m_4^2 \ .$$